# Task 6: Effect of Improved PBL on CAMx Ozone Prediction and Source Attribution

AQRP Project 24-021

Improving WRF Representation of Coastal, Marine, and Residual Boundary Layers and Quantifying the Effects on Ozone Prediction

Prepared by

Yuxuan Wang, University of Houston

James Flynn, University of Houston

July 1, 2025

## 1. Introduction

The previous tasks of the project conducted multiple perturbation simulations of the Weather Research and Forecasting (WRF) model version 4.6.0 by fine-tuning key parameters and constants in the Mellor-Yamada-Nakanishi-Niino Level 2.5 (MYNN2) planetary boundary layer (PBL) scheme within the published ranges. Additional sensitivity simulations were also conducted by selecting different cloud and urban physics schemes, as the base WRF model exhibited unrealistic PBL features that were traced back to those configurations, and turning on the 1-D ocean mixed layer model in the WRF model which improves simulation of the diurnal variation of sea surface temperature (SST) and results in a better planetary boundary layer height (PBLH) prediction over the water. Through the comparison of the sensitivity experiments with the base simulation and with PBLH observations, three sets of simulations emerged as winners: PBLH14 (combination of the Urban Canopy Model (UCM) with New Simplified Arakawa-Schubert (NSAS) cumulus scheme), PBLH23 (NSAS and 1-D ocean mixed layer model), and PBLH24 (PBLH14 plus the 1-D ocean mixed layer model). All three perturbation simulations yield better marine PBLH estimates than the base model (by increasing PBLH up to 400 m) when the observed PBLH values are high offshore, while having little effect on performance over land. When the observed PBLH values are low, mostly over the Gulf of America, the perturbation simulations show little difference compared to the base model. In the present task (Task 6), we focused on PBLH23 and PBL24, as PBL14 settings are included in PBLH24, to conduct further analysis, including an evaluation against independent PBL observations from a field campaign off the coast of Louisianna, and used these PBL perturbation simulations to drive the photochemical model, the Comprehensive Air Quality Model with extensions (CAMx).

The main objective of Task 6 is to understand the effects of improved PBL on ozone prediction and source attribution in the Houston-Galveston-Brazoria (HGB) region. To this end, we conducted CAMx v7.31 simulations driven by meteorological fields from the selected PBL perturbation simulations (PBLH23 and PBLH24) and quantified the resulting changes in CAMx-predicted surface ozone concentrations as compared to those CAMx outputs using the base WRF v4.6.0 model. Ozone predictions from the different simulations were also evaluated against Tracking Aerosol Convection ExpeRiment-Air Quality (TRACER-AQ) field campaign data to evaluate the extent to which improved PBL simulations affect the evaluation statistics of CAMx ozone prediction. The base CAMx simulation (i.e., CAMx driven by the base WRF v4.6.0 model) was also compared with our previous base CAMx simulations using an earlier version of WRF and CAMx to assess the differences caused by model version updates.

Ozone source attribution was previously estimated based on CAMx emission perturbation experiments during the September 2021 period., 80% of ozone in offshore locations around the HGB was attributed to regional background and a 10% reduction in local anthropogenic emissions of NOx and VOCs would result in only a 0.5% change in offshore ozone levels

(AQRP 22-008). These estimates are model-derived quantities and thus depend on the model settings. In Task 6, we examined this sensitivity due to PBL by conducting the same emission perturbation experiments using CAMx driven by the base WRF and selected PBL perturbation simulations.

## 2. Overview of WRF and Selected PBL Perturbation Simulations

The Weather Research and Forecasting (WRF) model version 4.6.0 with the Advanced Research WRF (ARW) solver was employed to simulate meteorological fields for three domains (**Figure 1**) over the contiguous United States (d01 - 12km×12km), Southeast Texas (d02 - 4km×4km), and the Houston-Galveston-Brazoria region (d03 - 1.33km×1.33km), respectively. All three domains have identical vertical resolutions with 30 vertical levels from the surface to ~100 hPa. As the base WRF configurations, we used the local closure Mellor-Yamada-Nakanishi-Niino Level 2.5 (MYNN2) PBL scheme (Nakanishi & Niino, 2009), Morrison double moment (2M) microphysics scheme (Morrison et al., 2009), Rapid Radiative Transfer Model (RRTMG) longwave and shortwave radiation schemes (Iacono et al., 2008), Monin-Obukhov similarity surface layer scheme (Chen et al., 1997), Noah land-surface module (Chen & Dudhia, 2001), and the New Tiedtke cumulus parameterization (Tiedtke, 1989; Zhang et al., 2011). The initial and boundary conditions (IC/BC) for domain d01 were derived from the High-Resolution Rapid Refresh (HRRR) model, while the IC/BC for d02 were generated from d01, and those for d03 were generated from d02. These configurations were selected from our previous work that yielded the best prediction of overall meteorological conditions (Liu et al., 2023) during the Tracking Aerosol Convection ExpeRiment-Air Quality (TRACER-AQ) field campaign period that took place from July – October 2021(TAQ1) (Jensen et al., 2021). In the present study, we expanded the evaluation by incorporating observational data from all three TRACER-AQ field campaigns: TAQ1 (July to October 2021), TAQ2 (April to October 2022), and TAQ3 (May to October 2023). The red lines in domain d03 (**Figure 1**) represent the mobile platform sampling tracks from these campaigns.

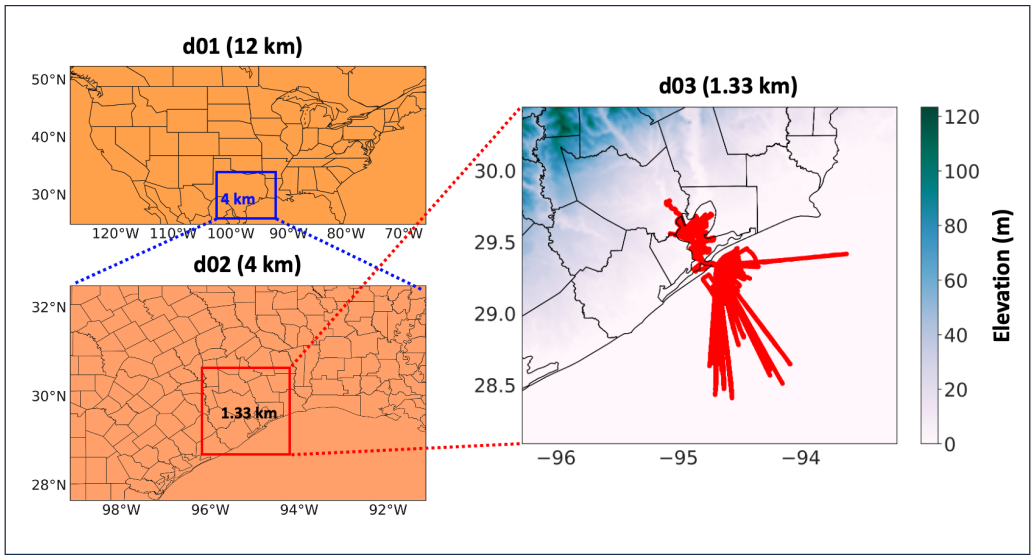


**Figure 1** WRF domains showing d01 (contiguous United States), d02 (Southeast Texas), and d03 (Houston-Galveston-Brazoria) regions. Red lines in d03 are the locations of ship-based measurements from University of Houston Pontoon Boat (UHPB), Red Eagle boat (RE), and Osprey Boat (OB) for the selected months.

Among the different perturbation and sensitivity simulations conducted in Task 4 and Task 5, PBLH23 and PBLH24 were selected as the two best-performing meteorological configurations for further analysis. These configurations were chosen based on their ability to improve the simulation of PBLH, particularly over the Houston-Galveston-Brazoria (HGB) region and adjacent coastal waters. PBLH23 includes the 1-D ocean mixed layer model and uses the New Simplified Arakawa-Schubert (NSAS) cumulus scheme. PBLH24 builds upon PBLH23 by additionally enabling the Urban Canopy Model (UCM) to better represent urban surface processes. These two configurations were selected for CAMx sensitivity simulations due to their superior performance in capturing marine boundary layer structure and improving agreement with observed meteorology and PBLH. For example, looking at temperature and PBLH from the University of Houston (U of H) Pontoon boat during September 2022, all three of the perturbation schemes outperformed the base model when compared to the observed data by having lower bias and capturing more variability of the observations. For PBLH, as shown in **Figure 2a**, PBLH14 performed worse with PBLH23 and PBLH24 showing similar performance. For temperature, as shown in **Figure 2b**, all perturbation schemes (PBLH14, 23, and 24) were similar to each other and outperformed the base run.

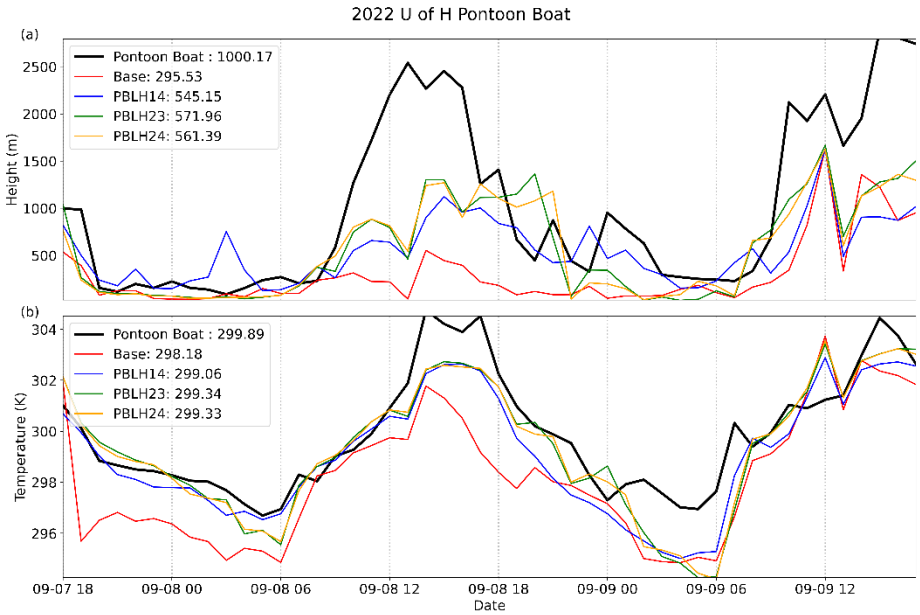


**Figure 2** (a) PBLH (m) and (b) Temperature (K) for observation data from the U of H Pontoon Boat (black), Base run (red), PBLH14 (blue), PBLH23 (green), and PBLH24 (orange) for September 2022.

## 3. Evaluation of PBL by SCOAPE Campaign Observations

Given the similarity between PBLH23 and PBLH24 in configuration and performance over the water, we chose the PBLH24 to be further evaluated by independent PBL measurements over the South Louisiana/Gulf of America from the Satellite Coastal and Oceanic Atmospheric Pollution Experiment (SCOAPE) 2019 (SCOAPE-19) campaign (Thompson et al., 2023). The SCOAPE-19 campaign was run in May 2019 and was composed of onshore and offshore observations. This report used only the offshore observations from the University of Southern Mississippi's Research Vessel (R/V) Point Sur, which cruised in the Gulf of America from the 10$^{th}$ to the 18$^{th}$ of May 2019 as this was the only observation that gave directly calculated PBLH. The PBL calculation was done automatically from the Lufft Cloud Height Meter (CHM) 8k ceilometer on board the R/V Point Sur and gave the heights of three PBLs per measurement. Only the first/lowest layer was used and was run through a filter to remove any possible artifacting and to temporally average the data per hour as shown in **Figure 3**b. High noise between 05-14 18:00 to 05-16 06:00 was present in the unfiltered observed data (**Figure 3a**). Due to the PBLH values being calculated from the integrated controller and the widespread presence of noise around that time, we think that this could be caused either by an instrument issue or an issue with the integrated controller. This period was removed from the analysis.

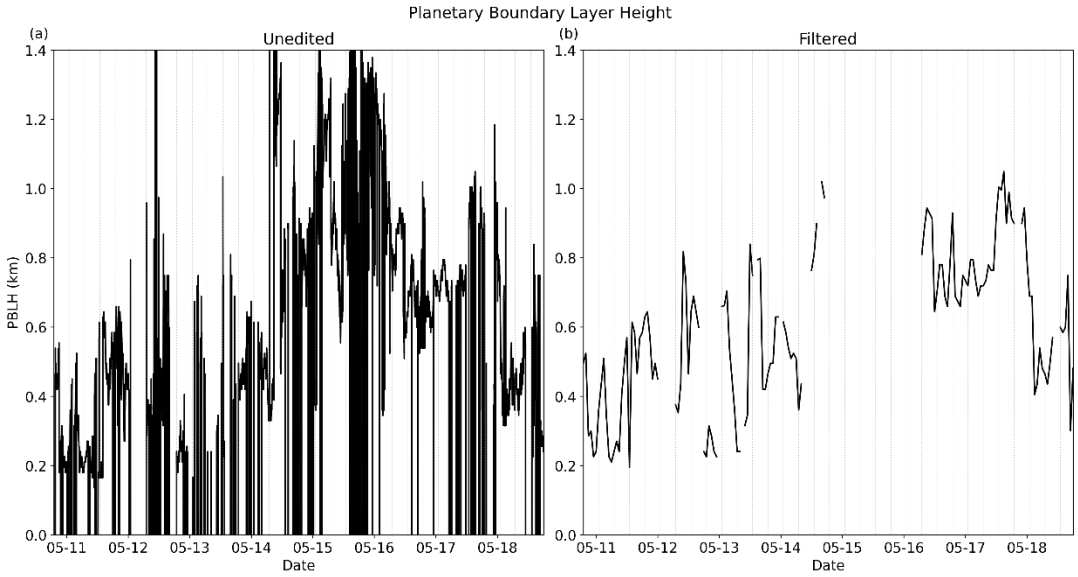


**Figure 3** (a) Unprocessed layer 1 PBLH (km) data and (b) Filtered PBLH (km) data from the Lufft CHM 8k ceilometer on board the R/V Point Sur in 2019.

The WRF v4.6.0 model, as described above, was set up for the SCOAPE campaign area as shown in **Figure 4**. The three domains are over the contiguous United States (d01 – 12 km x 12km), Southeastern Texas/Louisiana (d02 – 4kmx4km), and Southern Louisiana (d03 – 1.33 km x 1.33km), respectively. Two different model runs were done, the base model and a run using the settings from PBLH24 (PBLH24). The initial and boundary conditions (IC/BC) were generated in the same way as in Task 4, such that IC/BC for domain d01 were generated from the HRRR meteorology model, and IC/BC conditions for domains d02 and d03 were generated from d01 and d02, respectively. Both WRF runs were run from May 10th, 2019, to May 18th, 2019, with May 10th used as a spin-up day.

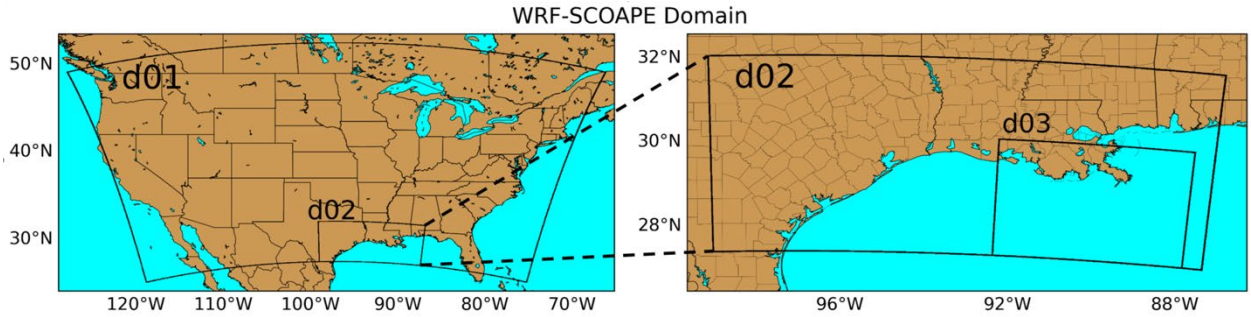


**Figure 4** WRF domains for SCOAPE showing d01 (contiguous United States), d02 (Southeastern Texas/Louisiana), and d03 (Southern Louisiana).

The performance of PBLH for both the base run and PBLH24 were evaluated by comparing to the filtered observation data from R/V Point Sur over the campaign period. Both the filtered observation data and WRF simulations have a temporal resolution of an hour. The model PBL values were taken based on the average latitude and longitude for each hour of the R/V Point Sur tracks.

Observed and simulated PBLH values are shown in **Figure 5** for the diurnal and in **Figure 6** over the track of R/V Point Sur. As observed in **Figure 5**, the diurnal profile of PBLH over the track of R/V Point Sur is relatively consistent with mean values ranging from ~0.5 km to ~0.8 km. Both models tend to overestimate early morning hours (3:00 – 10:00) while keeping close to the observed for the remainder of the hours. The base model's overestimation also correlates with its higher day-to-day variation, as denoted by the large color bars in **Figure 5**. PBLH24 has a lower bias and smaller day-to-day variation than the base model in the morning hours, making it better match the observations. The two models are similar in performance in the afternoon hours, while PBLH24 has a slower rate of PBL decreasing from late afternoon to the evening hours (18:00 – 20:00), like the observations.

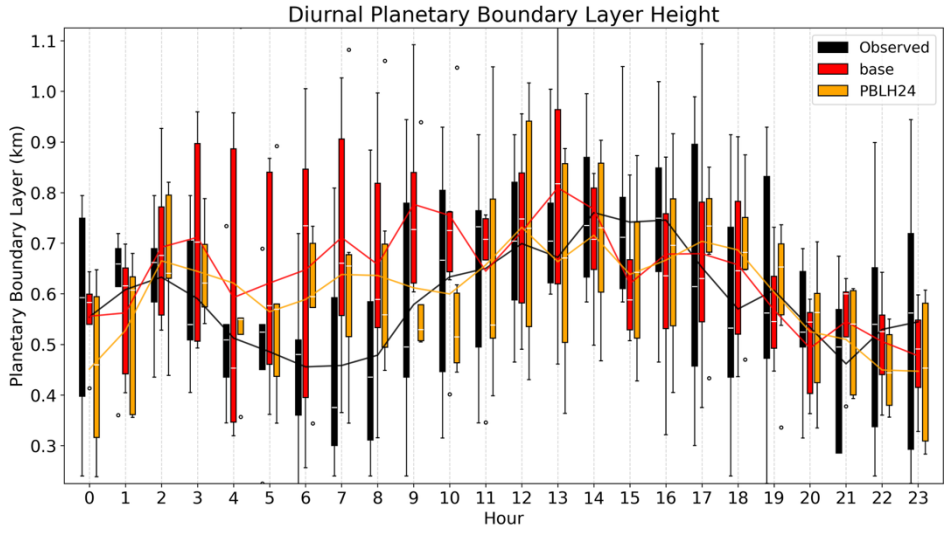


**Figure 5** Boxplot of the diurnal variation of PBLH over the ship track of R/V Point Sur for observed data (black), base run (red), and PBLH24 (orange). Data is from 05-10 19:00 to 05-18 19:00, with 05-14 18:00 to 05-16 06:00 removed.

Overall performance of the models is quite similar with the mean PBLH values of both WRF runs being within 50 m of each other (0.648 km and 0.611 km for base and PBLH24, respectively) as seen in **Figure 6**. When compared to the mean observed values, both runs are within 100 m, and both tend to slightly overestimate PBLH, with PBLH24 outperforming the base model by lowering the bias by 0.037 km. When looking at the correlation coefficient,

PBLH24 also shows a higher value (0.52) than the base run (0.43), showing better performance both spatially and temporally.

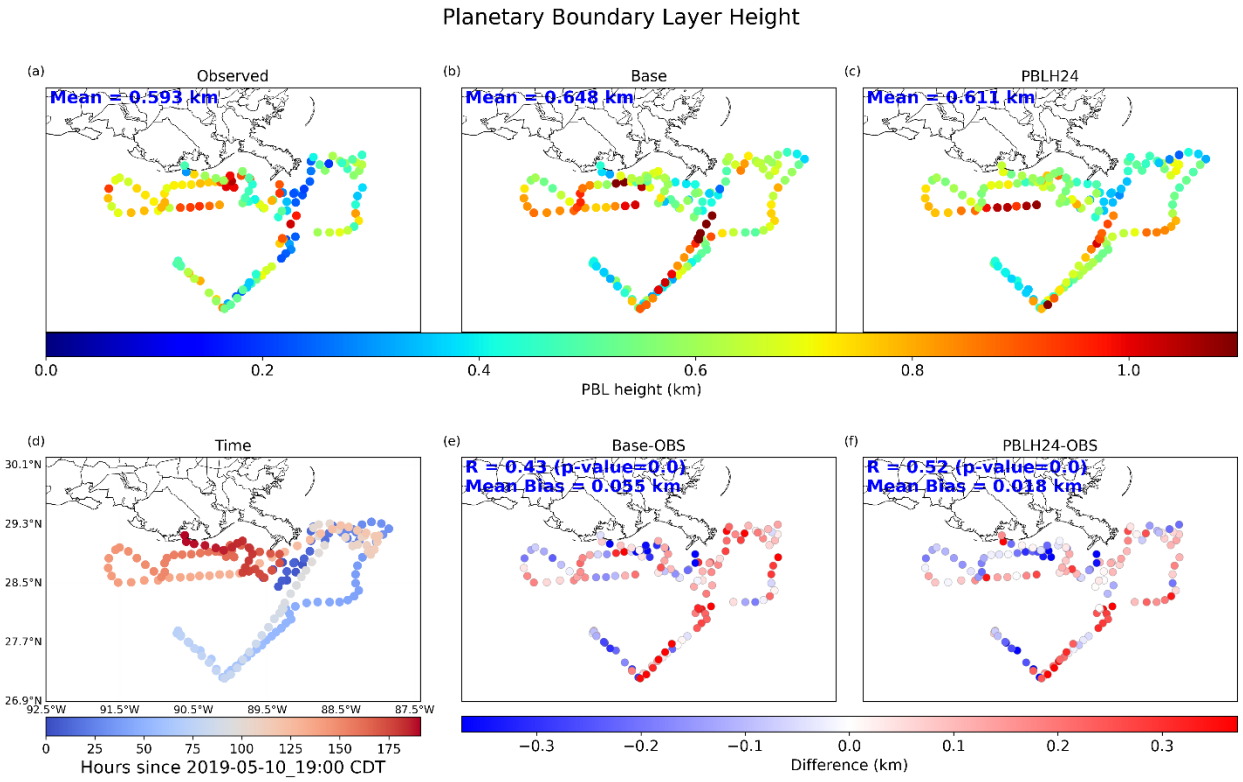


**Figure 6** PBLH over the R/V Point Sur ship track for (a) Observed, (b) Base run, (c) PBLH24 with time distribution shown in (d), and modeled-observed differences shown for the Base run (e) Base modeled-observed and (f) PBLH24-observed.

## 4. CAMx Configuration and Base Model Evaluation

Meteorological fields from WRF were directly used as the input to the Comprehensive Air Quality Model with extensions (CAMx) version 7.31 over d01, d02, and d03 domains. The initial and boundary conditions inputs for the d01 domain were obtained from the GEOS-Chem (v14.1.1) global simulation, while IC/BC for d02 and d03 were taken from d01 and d02, respectively. The first-order eddy viscosity (K-theory) diffusion scheme was selected for vertical mixing within the PBL, and the Carbon Bond version 6 revision 5 (CB6r5) was used for gas-phase chemistry (Burkholder et al., 2019). Dry deposition was implemented according to the Wesely scheme (Wesely, 2007). Anthropogenic emissions data from the 2019 State Implementation Plan (SIP) modeling platform provided by TCEQ were converted and used in the model as discussed in (Li et al., 2023). Biogenic emissions are generated from the Biogenic

Emission Inventory System (BEIS), and wildfire emissions are based on the Fire INventory from NCAR (FINNv2) from the SIP 2019 emission inventory.

The project team previously used CAMx version 7.10 in conjunction with meteorological inputs from WRF version 3.9.1.1 to simulate ozone photochemistry for the TAQ1 and TAQ2 campaigns (Li et al., 2023; Soleimanian et al., 2023). The present work used CAMx version 7.31, driven by meteorological fields from the more recent WRF version 4.6.0. We first assessed how version updates in both the meteorological and photochemical models affect ozone predictions over the HGB region.

**Figure 7** compares the time series of ozone concentrations simulated by CAMx v7.10 and v7.31 against boat observations for September 8–10, 2021, over Galveston Bay. CAMx v7.10 (green line), using WRF v3.9.1.1, produces higher peak ozone levels in the afternoon but overestimates morning and evening ozone, with a mean bias of +1.34 ppbv and a correlation coefficient (R) of 0.60 compared to the observations. In contrast, CAMx v7.31 (red line), using WRF v4.6.0, better captures the timing of ozone variability and the morning and evening ozone concentrations, with a slightly stronger correlation (R=0.64), but underestimates peak ozone levels and has a negative mean bias of -4.18 ppbv over the selected period (Sep 8-10, 2021). These results indicate that the updated WRF-CAMx system improves temporal representation but underpredicts peak ozone under certain conditions. The subsequent analysis and results in the report are based on CAMx v7.31, driven by meteorology from WRF v4.6.0, and the model version numbers will not be specified for simplicity. We refer to CAMx driven by the WRF base model as the CAMx base model, and those driven by the selected PBL perturbation simulations as CAMx-PBLH23 and CAMx-PBLH24, respectively.

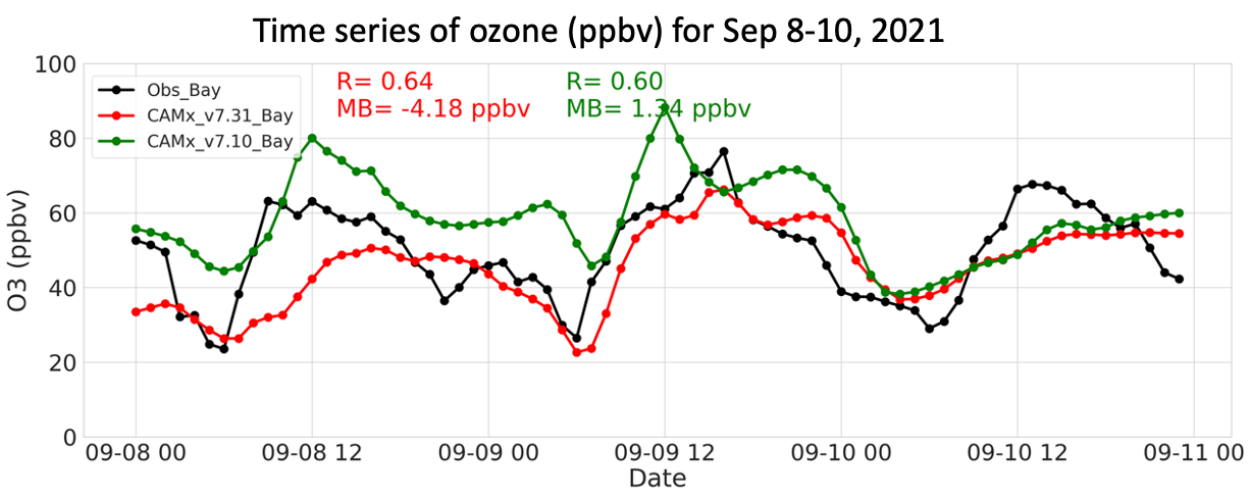


**Figure 7** Time series of ozone (ppbv) for September 8-10, 2021, over Galveston Bay. Black lines represent observed ozone, red lines show CAMx v7.31 simulations, and green lines show

CAMx v7.10 simulations. Statistical metrics (correlation, mean bias) are shown for each model version.

The evaluation of CAMx base model performance on ozone predictions focused on September 8-10 for 2021 and 2022 (**Figure 8)**. These dates represent both high ozone and clean periods, allowing us to assess model performance under varying air quality conditions. These dates also aligned with periods of available mobile boat observations during the TRACER-AQ campaigns. In 2021, the boat sampling was active primarily within Galveston Bay, so the evaluation for that year is limited to the Bay region. In 2022, the observational coverage expanded to include both Galveston Bay and the Gulf of America, providing a broader spatial domain for comparison. This contrast in measurement coverage between the two years allows for a more complete assessment of CAMx performance over the coastal and marine environment.

**Figure 8** presents the spatial distribution of observed and CAMx base-simulated ozone concentrations, along with the model-observation difference, for September 8-10, 2021, and 2022, over Galveston Bay and the Gulf of America. The plots include only daytime (07:00 to 19:00 CDT) mobile measurements to emphasize photochemically active periods and exclude nighttime docked observations, which are more influenced by land-based processes.

Over Galveston Bay in 2021, CAMx captured the general spatial gradient of ozone but tended to underestimate concentrations across most of the Bay, with a mean bias of -12.73 ppbv. The underestimation appears more pronounced during morning hours in the southern Bay, while in the afternoon the model slightly overestimated ozone in the northern Bay near the Houston Ship Channel (HSC). In 2022, CAMx showed regionally varying performance in the spatial variability of ozone across Galveston Bay, with a mean bias of -9.80 ppbv. Most of the sampling in the southern Bay occurred during afternoon hours, where the model tended to underestimate ozone in this more marine-influenced region. In northwestern Bay and around the HSC, the model often overestimated ozone in the afternoon, similar to the 2021 pattern.

Over the Gulf of America in 2022, CAMx slightly underestimated ozone throughout the boat route, with a mean bias of -4.77 ppbv. While the magnitude of the bias was smaller than over Galveston Bay, the model struggled to capture the observed variability, especially during afternoon sampling periods. This indicates potential limitations in representing ozone dynamics over open water under the current base model configuration.

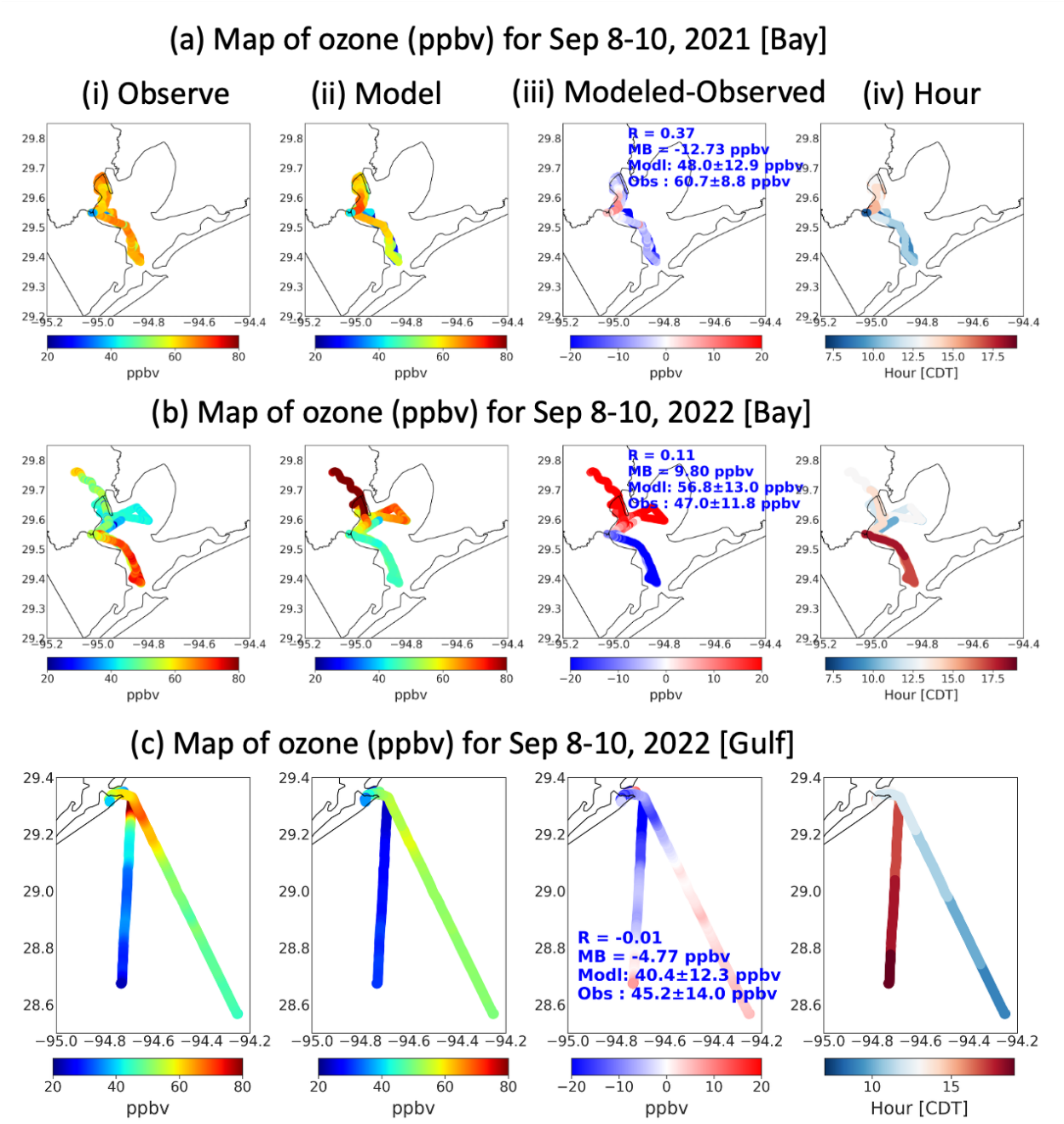


**Figure 8** (a) Map of the observed, CAMx base modeled, and modeled-observed ozone (ppbv) over Galveston Bay for September 8-10, 2021, along with the time/hour when the boat was mobile. (b) Same as (a), but for September 8-10, 2022. (c) Same as (b) but for the Gulf of America. The plot shows daytime (7:00 CDT – 19:00 CDT) mobile data only.

## 5. Effects of Improved PBL on CAMx Ozone Prediction

To evaluate the effect of improved PBL representation on ozone prediction, CAMx simulations were conducted using meteorology from the WRF base model as well as two best selected PBL perturbation configurations: PBLH23 and PBLH24. These simulations were performed for September 8-10 in both 2021 and 2022 and were compared to the CAMx base model as well as observed ozone concentrations from the TRACER-AQ mobile platform data over Galveston Bay and the Gulf of America.

**Figure 9** shows the average surface ozone concentrations simulated by the Base, PBLH23, and PBLH24 configurations for the selected periods. In both years, CAMx simulations driven by PBLH23 and PBLH24 produced higher average ozone surface concentrations compared to the base simulation, particularly over Galveston Bay and coastal regions. This increase in modeled ozone is associated with the deeper and more realistic PBL heights produced by PBLH23 and PBLH24. Enhanced vertical mixing over the water would both bring down ozone precursors from aloft (i.e., the sea breeze return flow) leading to increased photochemical production of ozone, and increase the entrainment of free-tropospheric ozone into the boundary layer.. Notably, PBLH24, which combines the urban canopy model (UCM), NSAS cumulus scheme, and the 1-D ocean mixed layer model, resulted in the most widespread ozone enhancement of ~10 ppbv on average across the whole domain. PBLH23, which has the same settings as PBLH24 except for the UCM, saw ozone increases mainly in offshore locations with an average of ~8 ppbv. The contrast between PBLH23 and PBLH24 suggests it is the UCM that leads to ozone increases over land.

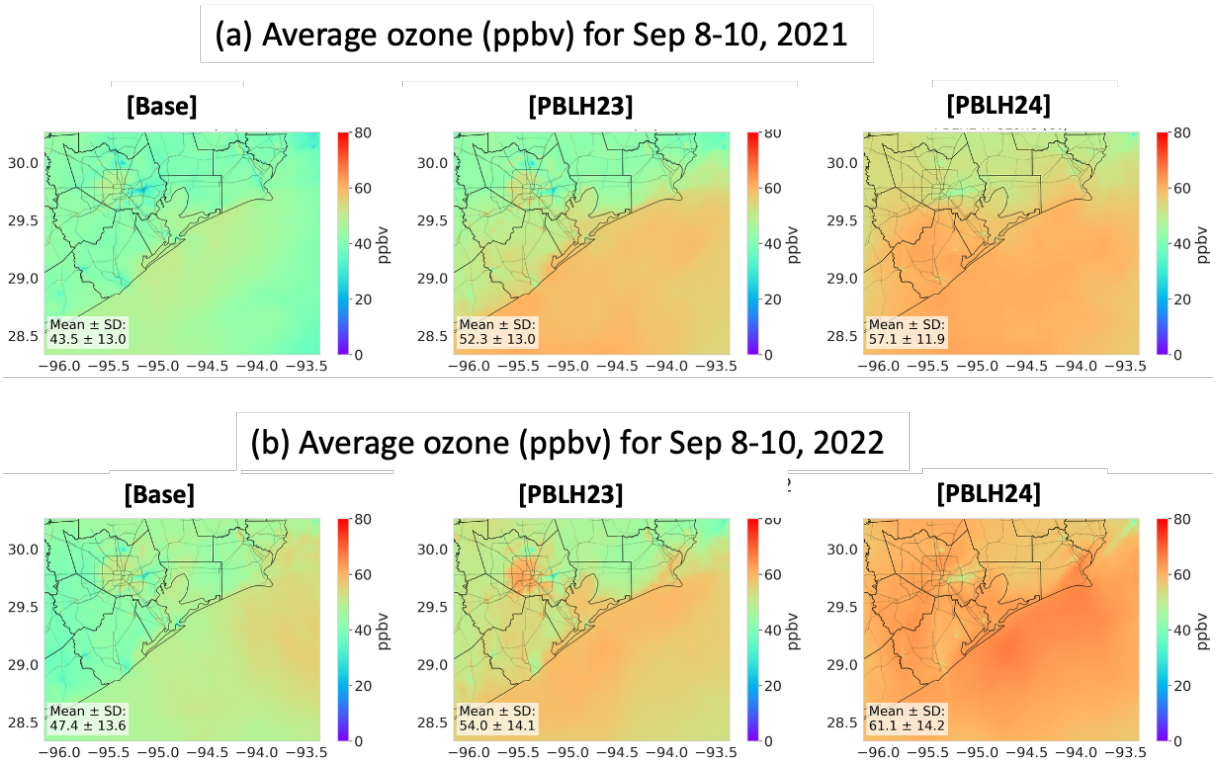


**Figure 9** Average ozone (ppbv) surface concentration for CAMx base, PBLH23, and PBLH4, for (a) September 8-10, 2021, and (b) September 8-10, 2022.

**Figure 10** compares the time series of observed and simulated ozone concentrations at the offshore sampling locations during Sep 8-10, 2021, and 2022 between the base, PBLH23, and PBLH24. Consistent with Figure 4, both PBLH23 and PBLH24 simulated higher ozone at the offshore locations than the base, eliminating the negative bias of the base simulation over Galveston Bay in 2021 (**Figure 10a**) and over the Gulf of America in 2022 (**Figure 10c**). However, over the Bay in 2022, where the base model had a positive bias of ~ 7 ppbv to begin with (**Figure 10b**), PBLH23 and PBLH24 produced a more severe positive bias of ~14 ppbv and 23 ppbv, respectively. Despite such an increase of the overall positive bias, PBLH23 predicted 10-15 ppbv lower ozone than the base during the early morning hours (~6:00 am) over the Bay on Sep 8 and Sep 9, 2022, which more closely aligns with the observed low values (**Figure 10b**). In terms of the model's spatiotemporal variability as indicated by the correlation coefficient (R), both PBLH23 and PBLH24 significantly outperform the base over the Bay and the Gulf for the 2022 sampling period. For example, R increased from ~0.3 in the base to 0.65-0.7 in PBLH23 and PBLH24 over the Gulf in 2022 (**Figure 10c**). Considering both the bias and variability over the offshore sampling locations, PBLH23 stands out as the winner in ozone prediction.

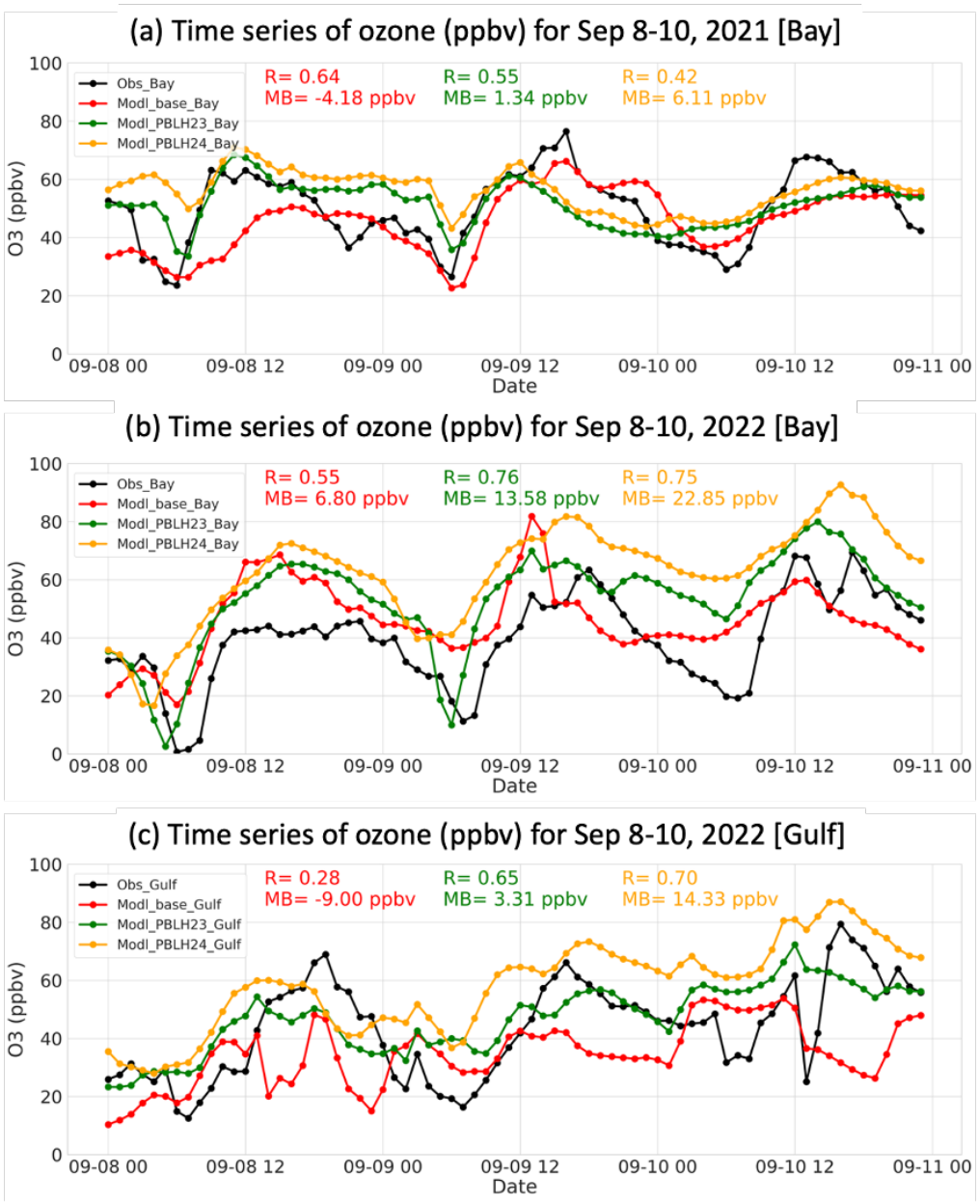


**Figure 10** (a) Time series of ozone (ppbv) for September 8-10, 2021, over Galveston Bay, (b) Same as (a) but for September 8-10, 2022, and (c) Same as (b) but for the Gulf of America. Black lines represent observed ozone, red lines show base simulation, green lines show PBLH23, and orange lines show PBLH24. Statistical metrics (correlation, mean bias) are shown for each plot.

## 6. Effects of Improved PBL on Regional vs. Local Contributions to Ozone

Background ozone refers to the surface ozone concentration in a region influenced primarily by long-range transport, biogenic emissions, and free-tropospheric entrainment, in the absence of local anthropogenic emissions. To estimate regional background ozone in the Houston-Galveston-Brazoria (HGB) area, we performed CAMx zero-emission simulations (referred to as the background [BGD] cases), in which all anthropogenic emissions were turned off within the innermost domain (d03). These simulations retained biogenic emissions and used the same meteorological and chemical boundary conditions as their corresponding full-emission control (CTR) runs. Background simulations were conducted for each meteorological configuration of CAMx: Base, PBLH23, and PBLH24, for September 8-10 in both 2021 and 2022. Comparing the BGD and CTR results allows us to quantify the contribution of anthropogenic emissions to surface ozone within the HGB region and assess how changes in meteorology influence background ozone levels.

**Figure 11** presents the daytime average (08:00–20:00 CDT) surface ozone for the CTR and BGD simulations across all three meteorological cases and both years. In 2021, for the Base simulation, the average surface ozone in the HGB region was 49.0 ppbv, while the background ozone was 40.1 ppbv, indicating that ~81.8% of the total ozone was attributed to regional background. These results are consistent with findings from previous work (AQRP Project 22-008), which also reported a dominant role of background processes over the HGB region. In PBLH23, the total ozone increased to 56.3 ppbv, and background ozone rose to 45.1 ppbv, resulting in a slightly lower relative background contribution of 80.1%. In PBLH24, total ozone further increased to 59.5 ppbv, with background ozone at 56.2 ppbv, yielding a background contribution of approximately 94.5%. This suggests that while PBLH24 substantially enhanced background ozone through stronger mixing and entrainment, it did not significantly increase the influence of local emissions in 2021. Unlike PBLH23 and the Base case, PBLH24 shows the least local anthropogenic impact under these conditions. Despite the difference in the predicted magnitude of local ozone, the spatial distribution of local ozone is similar between the two cases.

In 2022, the contribution of local anthropogenic emissions to total ozone varied across meteorological configurations. For the Base simulation, total ozone averaged 53.0 ppbv, while background ozone was 45.6 ppbv, indicating that ~ 86% of the total ozone was attributed to regional background. In PBLH23, total ozone increased to 59.9 ppbv, and background ozone to 48.2 ppbv, resulting in a background contribution of ~80.5%. In PBLH24, total ozone reached 66.3 ppbv, and background ozone was 54.7 ppbv, yielding a background contribution of ~82.5%. The results indicate that the improved vertical mixing in PBLH23 and PBLH24 increased not only the entrainment of ozone-rich air aloft (boosting background ozone) but also enhanced the surface impact of local anthropogenic emissions.

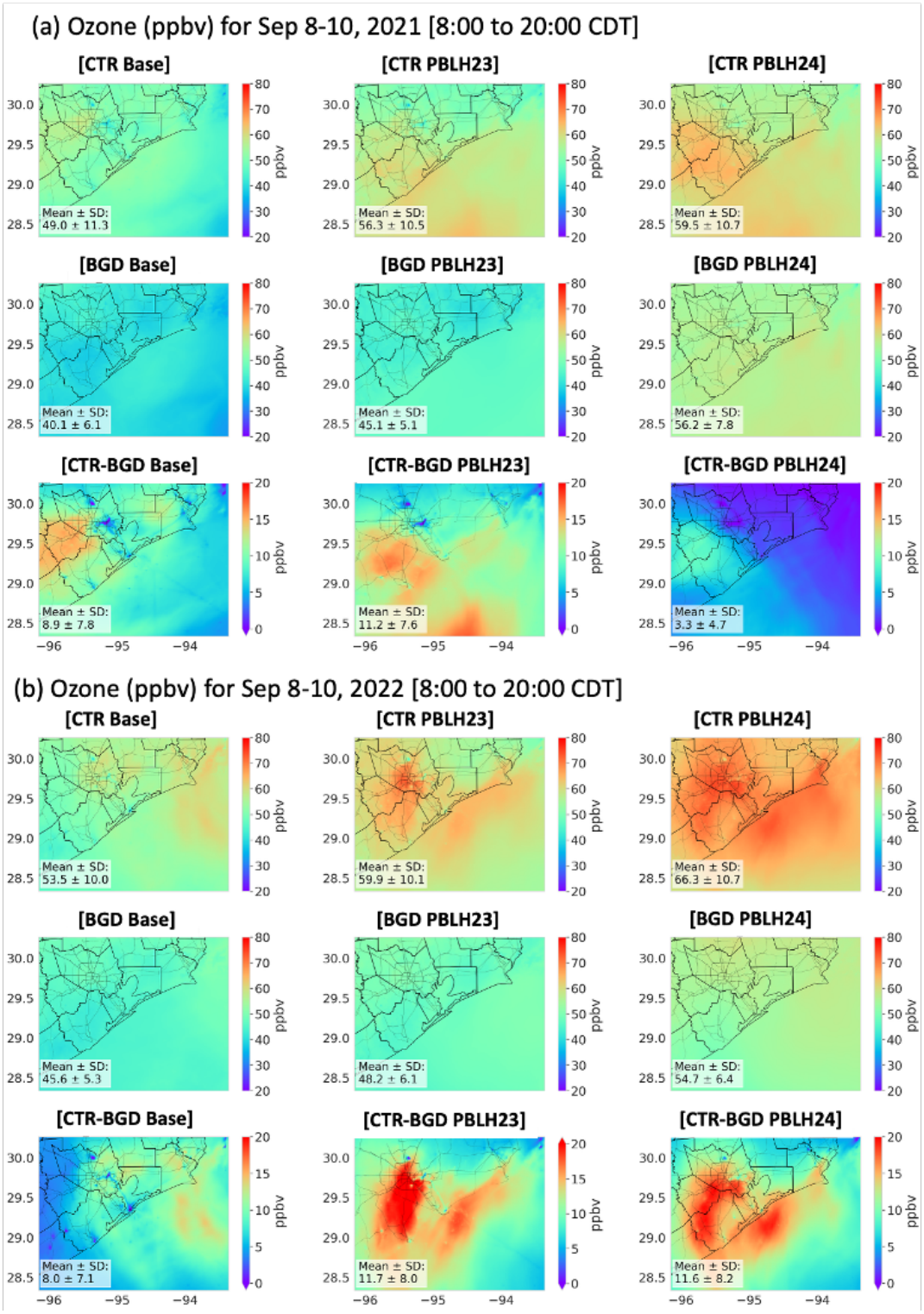
(a) Ozone (ppbv) for Sep 8-10, 2021 [8:00 to 20:00 CDT]
[CTR Base]
Mean ± SD:
49.0 ± 11.3
[CTR PBLH23]
Mean ± SD:
56.3 ± 10.5
[CTR PBLH24]
Mean ± SD:
59.5 ± 10.7
[BGD Base]
Mean ± SD:
40.1 ± 6.1
[BGD PBLH23]
Mean ± SD:
45.1 ± 5.1
[BGD PBLH24]
Mean ± SD:
56.2 ± 7.8
[CTR-BGD Base]
Mean ± SD:
8.9 ± 7.8
[CTR-BGD PBLH23]
Mean ± SD:
11.2 ± 7.6
[CTR-BGD PBLH24]
Mean ± SD:
3.3 ± 4.7
(b) Ozone (ppbv) for Sep 8-10, 2022 [8:00 to 20:00 CDT]
[CTR Base]
Mean ± SD:
53.5 ± 10.0
[CTR PBLH23]
Mean ± SD:
59.9 ± 10.1
[CTR PBLH24]
Mean ± SD:
66.3 ± 10.7
[BGD Base]
Mean ± SD:
45.6 ± 5.3
[BGD PBLH23]
Mean ± SD:
48.2 ± 6.1
[BGD PBLH24]
Mean ± SD:
54.7 ± 6.4
[CTR-BGD Base]
Mean ± SD:
8.0 ± 7.1
[CTR-BGD PBLH23]
Mean ± SD:
11.7 ± 8.0
[CTR-BGD PBLH24]
Mean ± SD:
11.6 ± 8.2
ppbv
30.0
29.5
29.0
28.5
−96
−95
−94

**Figure 11** Daytime average (08:00–20:00 CDT) surface ozone concentrations (ppbv) from CAMx simulations for (a) September 8-10, 2021, and (b) September 8-10, 2022. Each panel includes three columns corresponding to the Base, PBLH23, and PBLH24 meteorological configurations. The first row shows control (CTR) simulations with full anthropogenic and biogenic emissions, the second row shows background (BGD) simulations with anthropogenic emissions turned off, and the third row shows the difference between control and background (CTR − BGD), representing the modeled contribution of local anthropogenic emissions to surface ozone.

Overall, these findings demonstrate that meteorological conditions and PBL structure significantly affect the estimation of regional background and local emissions on ozone in the HGB region. While simulations with enhanced marine PBL representation (PBLH23 and PBLH24) increased absolute background ozone due to stronger vertical mixing and entrainment, they also amplified the surface influence of local anthropogenic emissions. A notable difference between the two years is that local emissions contributed a greater fraction to surface ozone in 2022 compared to 2021 across all configurations. For example, in the PBLH24 case, anthropogenic contributions increased from 5.5% in 2021 to 17.5% in 2022, suggesting that more active photochemical conditions and meteorological variability in 2022 made the region more responsive to local precursor emissions.

## 7. Conclusions

This study evaluates the impact of improved planetary boundary layer height representation on CAMx ozone predictions and source attribution for the Houston-Galveston-Brazoria (HGB) region, focusing on the period of September 8-10 for both 2021 and 2022. The work builds on earlier efforts (Tasks 4 and 5) and uses meteorological inputs from the WRF v4.6.0 model under three configurations: a Base, and two improved configurations, PBLH23 and PBLH24, which were selected from prior perturbation/sensitivity experiments for their better performance in simulating PBLH over the water. Meteorological inputs from the WRF base model as well as these improved PBLH cases were used to drive CAMx v7.31 simulations to assess the influence of boundary layer dynamics on surface ozone distribution and source contributions.

Evaluation of the CAMx base simulation showed a tendency to underestimate surface ozone over Galveston Bay and the Gulf of America, particularly during morning and early afternoon hours. In contrast, simulations using the PBLH23 and PBLH24 configurations produced higher ozone levels, improved spatial variation, and significantly reduced model bias. PBLH24 led to the largest overall ozone enhancement, especially over land, due to the inclusion of the Urban Canopy Model (UCM), while PBLH23 showed better balance by reproducing low ozone in the early morning and minimizing afternoon overestimations. Overall, both improved cases outperformed the base, with PBLH23 showing better overall ozone prediction.

To estimate the contributions of regional background and local anthropogenic emissions, zero-emission simulations were performed. Background ozone increased with improved PBL representation due to enhanced vertical mixing and entrainment of ozone-rich air. In 2021, local contributions remained low, especially in PBLH24, where only 5.5% of total ozone was attributed to anthropogenic sources. In 2022, however, local contributions were higher in all scenarios, with PBLH23 showing the strongest local influence (~19.5%), reflecting more active photochemistry and a greater sensitivity to local emissions.

In summary, this work highlights the importance of meteorology, particularly the structure of the PBLH, in driving ozone variability and source attribution in coastal environments. Improved PBLH configurations not only enhanced model agreement with observations but also shifted the balance between background and locally produced ozone. Among the tested configurations, PBLH23 provided the best trade-off between bias reduction and realistic attribution of local versus regional contributions.

Subsequent work of the project will examine the ozone responses to the PBL perturbation configurations (e.g, PBLH23 and PBLH24) in more detail, such as by comparing to routine surface ozone monitors and adding more simulation days to cover different conditions (e.g., high ozone periods in September 2023). We will also implement the residual layer estimation method developed in Task 5 in the CAMx perturbation simulations to investigate how the improved PBLH configurations affect the vertical mixing of ozone and ozone precursors between the residual layer (RL) and the free troposphere and between the RL and the surface.

**Reference:**

Burkholder, J. B., Sander, S. P., Abbatt, J., Barker, J. R., Cappa, C., Crounse, J. D., Dibble, T. S., Huie, R. E., Kolb, C. E., Kurylo, M. J., Orkin, V. L., Percival, C. J., Wilmouth, D. M., & Wine, P. H. (2019). Chemical kinetics and photochemical data for use in atmospheric studies, Number 19. In *Jet Propulsion Laboratory, Pasadena: Vol. JPL Public* (Issue II).

Chen, F., & Dudhia, J. (2001). Coupling an advanced land surface–hydrology model with the Penn State–NCAR MM5 modeling system. Part I: Model implementation and sensitivity. *Monthly Weather Review*, *129*(4), 569–585.

Chen, F., Janjić, Z., & Mitchell, K. (1997). Impact of atmospheric surface-layer parameterizations in the new land-surface scheme of the NCEP mesoscale Eta model. *Boundary-Layer Meteorology*, *85*(3), 391–421.

Iacono, M. J., Delamere, J. S., Mlawer, E. J., Shephard, M. W., Clough, S. A., & Collins, W. D. (2008). Radiative forcing by long-lived greenhouse gases: Calculations with the AER radiative transfer models. *Journal of Geophysical Research: Atmospheres*, *113*(D13).

Jensen, M. P., Flynn, J. H., Judd, L. M., Kollias, P., Kuang, C., McFarquhar, G., Nadkarni, R., Powers, H., & Sullivan, J. (2021). A Succession of Cloud, Precipitation, Aerosol, and Air Quality Field Experiments in the Coastal Urban Environment. *Bulletin of the American Meteorological Society*, *102*(2). https://doi.org/10.1175/BAMS-D-21-0104.1

Li, W., Wang, Y., Liu, X., Soleimanian, E., Griggs, T., Flynn, J., & Walter, P. (2023). Understanding offshore high-ozone events during TRACER-AQ 2021 in Houston: Insights from WRF-CAMx photochemical modeling. *Atmospheric Chemistry and Physics*, *23*(21). https://doi.org/10.5194/acp-23-13685-2023

Liu, X., Wang, Y., Wasti, S., Li, W., Soleimanian, E., Flynn, J., Griggs, T., Alvarez, S., Sullivan, J. T., Roots, M., Twigg, L., Gronoff, G., Berkoff, T., Walter, P., Estes, M., Hair, J. W., Shingler, T., Scarino, A. J., Fenn, M., & Judd, L. (2023). Evaluating WRF-GC v2.0 predictions of boundary layer height and vertical ozone profile during the 2021 TRACER-AQ campaign in Houston, Texas. *Geoscientific Model Development*, *16*(18). https://doi.org/10.5194/gmd-16-5493-2023

Morrison, H., Thompson, G., & Tatarskii, V. (2009). Impact of cloud microphysics on the development of trailing stratiform precipitation in a simulated squall line: Comparison of one-and two-moment schemes. *Monthly Weather Review*, *137*(3), 991–1007.

Nakanishi, M., & Niino, H. (2009). Development of an improved turbulence closure model for the atmospheric boundary layer. *Journal of the Meteorological Society of Japan. Ser. II*, *87*(5), 895–912.

Soleimanian, E., Wang, Y., Li, W., Liu, X., Griggs, T., Flynn, J., Walter, P. J., & Estes, M. J. (2023). Understanding ozone episodes during the TRACER-AQ campaign in Houston, Texas: The role of transport and ozone production sensitivity to precursors. *Science of the Total Environment*, *900*. https://doi.org/10.1016/j.scitotenv.2023.165881

Tiedtke, M. (1989). A comprehensive mass flux scheme for cumulus parameterization in large-scale models. *Monthly Weather Review*, *117*(8), 1779–1800.

Wesely, M. L. (2007). Parameterization of surface resistances to gaseous dry deposition in regional-scale numerical models. *Atmospheric Environment*, *41*, 52–63.

Zhang, C., Wang, Y., & Hamilton, K. (2011). Improved representation of boundary layer clouds over the southeast Pacific in ARW-WRF using a modified Tiedtke cumulus parameterization scheme. *Monthly Weather Review*, *139*(11), 3489–3513.